

Study on Performance of Multi-user MRR Laser Communication in Atmospheric Turbulence Fading

Gaosi Li^a, Jian Geng^a, Yongsheng Cheng^a, Tianqi Gu^b

^aBeijing Institute of Space Long March Vehicle;

^bChina Academy of Launch Vehicle Technology

ABSTRACT

With the advantages of high communication rate and strong anti-interference, wireless laser communication is very suitable for space BPV communication, UAV directional communication and other scenarios with large-volume data and high reliability requirements. In order to break the traditional one-to-one laser communication scenario, a multi-user modulating retro-reflector(MRR) laser communication system is proposed in this paper, while ensuring the miniaturization of the receiver equipment and realizing multi-user cascade communication. The closed form solution of the outage probability of the proposed multi-user MRR laser communication system under atmospheric turbulence fading is derived, and the influence of system parameters on the system performance is analyzed. The correctness of the derived results is verified by simulation results.

Keywords: wireless laser communication, modulating retro-reflector, multi-user, outage probability.

1. INTRODUCTION

Wireless laser communication(WLC), also called free space optical communication(FSO), is a newly emerging communication technology using laser as a carrier, with the advantages of large communication capacity, high information transmission rate, high confidentiality, strong anti-interference, which can be employed in the satellite communication, satellite-ground communication, underwater communication and ground communication[1-2]. It will play an effective role in ship communication, mine communication and other scenes that are difficult to establish communication with traditional communication[3]. WLC can be divided into atmospheric laser communication, deep space laser communication and underwater laser communication according to different transmission media, and it can also be divided into satellite laser communication, ground laser communication according to different application scope[4]. As the laser transmitting angle is very small, the transmitting equipment and receiving equipment of the traditional space optical communication system need to be equipped with complex acquisition and tracking systems, which will significantly increase the weight, power consumption and volume of the communication system and make the traditional laser communication system unable to be used in the situation of miniaturization and low power consumption. Obviously, the size power limitations restrict the development of WLC[5]. The basic principle of MRR WLC is to modulate the incident light through the reverse end and then return to the transmitting equipment by the original path to achieve communication, eliminating the tracking and transmitting system of the traditional receiving terminal, effectively reducing the size of the laser communication system. Meanwhile, as the power consumption required by the reverse end is low, the MRR WLC can be used in micro platforms[6-7].

Atmospheric turbulence fading is one of the main disturbances that affect the performance of WLC. In academia, researchers have proposed many discrete statistical models to simulate the atmospheric turbulence fading process. The Gamma-Gamma model is closely concerned because of its strong consistency with the measured data[8]. In [9-10], the researchers analyzed the influence of atmospheric turbulence. Considering the influence of atmospheric turbulence, the performance of WLC will degrade conspicuously[11-14]. However, the research on the performance of MRR WLC is mostly focused on the performance analysis under the influence of weak turbulence, and only some researchers have studied the performance of communication systems that can adapt to the change of atmospheric turbulence intensity varying from weak to strong[15].

In this paper, the scene of multi-user MRR WLC in atmospheric turbulence fading is studied. Compared with the traditional WLC, the scene proposed in this paper breaks the limit of one-to-one communication and realizes communication between the transmitter and the receivers in different directions by design of incident and output angels of the reverse ends, which expands the applicable scenarios of WLC. Meanwhile, according to analysis of the outage probability in multi-user MRR WLC system, the effect of different user number is discussed. The analysis result is proved by simulation results.

The remaining of the paper is organized as follows. The scene of multi-user MRR WLC in atmospheric turbulence fading is introduced in Section II, together with the probability density function expression with Gamma-Gamma channel model. In Section III, the outage probability of the proposed system model is derived, and the parameters that have an effect on the outage probability is analyzed. The simulation results, which verify the correctness of derived results, are present in Section IV. Conclusions are drawn in Section V.

2. SYSTEM MODEL

In this paper, the system model shown in Figure 1 is considered, which contains 1 transmitter and N receivers. The transmitter has a laser transceiver, and each receiver is equipped with the MRR devices. The receivers set the laser incidence direction and outage direction according to the spatial positions of front and backward communication nodes, completing the cascade communication between transmitter and receivers. During communication, the transmitter inserts a synchronization mark in the laser signal, and each receiver carries out MRR in different laser areas to complete the communication, which shown in Figure 2. In order to ensure that each receiver has enough information processing time, it is agreed that each receiver will reverse modulate the laser in the laser return phase instead of the incident phase.

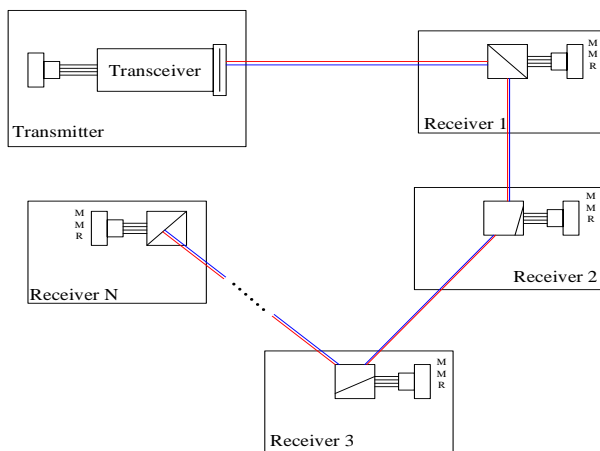


Figure 1. Multi-user MRR Laser Communication System Diagram

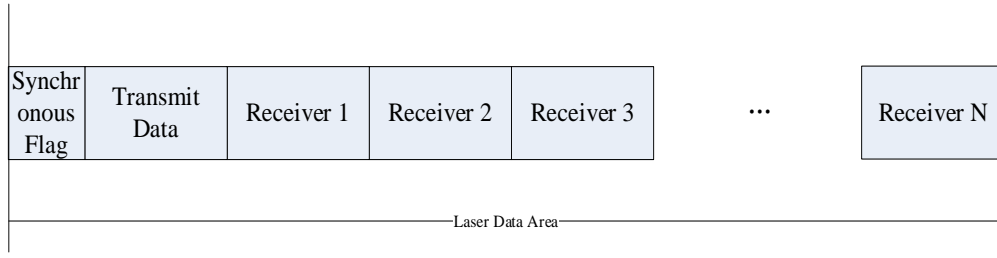


Figure 2. MRR Laser Communication Data Area Allocation Diagram

According to the system model in Fig.1, it can be known that the receive laser signal of the laser transceiver can be expressed as,

$$y = \eta h I S + n \quad (1)$$

where I is the light intensity when sending bit '1', $S \in \{0,1\}$ is the desired data, $n \in CN(0, \sigma_n^2)$ is the additive white Gaussian noise, η is the photoelectric conversion coefficient and h is the MRR channel fading, which can be expressed as,

$$h = h_a^{2N-1} h_{0,1} h_{1,2} \cdots h_{N-1,N} h_{N,N-1} \cdots h_{1,0} \quad (2)$$

where $h_{j-1,j}$ and $h_{j,j-1}$ represent the random attenuation of atmospheric turbulence in the forward link and the backward link between the receiver $j-1$ and the receiver j , respectively (the subscript '0' is stand for the transmitter). h_a is the fixed attenuation of the system [16], and in this paper, the fixed attenuation in forward link and backward link between the receivers is assumed to be same.

While the Gamma-Gamma model is used to describe the random attenuation of atmospheric turbulence in forward link and backward link, the probability density functions of $h_{j-1,j}$ and $h_{j,j-1}$ can be written as equation (3),

$$f_{h_{i,j}}(h_{i,j}) = \frac{2(\alpha_{i,j}\beta_{i,j})^{\frac{\alpha_{i,j}+\beta_{i,j}}{2}}}{\Gamma(\alpha_{i,j})\Gamma(\beta_{i,j})} h_{i,j}^{\frac{\alpha_{i,j}+\beta_{i,j}-1}{2}} K_{\alpha_{i,j}-\beta_{i,j}}(2\sqrt{\alpha_{i,j}\beta_{i,j}h_{i,j}}) \quad (3)$$

where $K_v(\cdot)$ represents the second-class Bessel function. $\alpha_{i,j}$ and $\beta_{i,j}$ are large-scale fading coefficient and small-scale fading coefficient of the Gamma-Gamma model, respectively. In MRR system, the two coefficients are related to the laser aperture size of receivers, communication distance and laser wavelength, and can be expressed as,

$$\alpha_{i,j} = \left\{ \exp\left[\frac{0.49\delta_{i,j}^2}{(1+0.65d_{i,j}^2+1.11\delta_{i,j}^{12/5})^{7/6}} \right] - 1 \right\}^{-1}$$

$$\beta_{i,j} = \left\{ \exp\left[\frac{0.51\delta_{i,j}^2(1+0.69\delta_{i,j}^{12/5})^{-5/6}}{1+0.9d_{i,j}^2+0.62d_{i,j}^2\delta_{i,j}^{12/5}} \right] - 1 \right\}^{-1} \quad (4)$$

where $d_{i,j} = \sqrt{kD_j^2/(4L_{i,j})}$. D_j is the aperture size of receiver j , $L_{i,j}$ is the communication distance between receiver i and receiver j , $k = 2\pi/\lambda$ is the laser wavenumber, λ is the laser wavelength, and $\delta_{i,j}^2$ is Litov variance, which can be expressed as,

$$\delta_{i,j}^2 = 1.23C_n^2 k^{7/6} L_{i,j}^{11/6} \quad (5)$$

where C_n^2 is the atmospheric refractive index structure constant. Under normal conditions, $C_n^2 = 1.7 \times 10^{-14} m^{-2/3}$ during the day time, and $C_n^2 = 8.4 \times 10^{-15} m^{-2/3}$ at night.

3. CALCULATION OF COMMUNICATION PERFORMANCE

In this section, the outage probability of the proposed multi-user laser communication system is considered to be the evaluation criteria of the system performance. The outage probability is defined as equation (6),

$$P_{out} = \Pr\{\gamma \leq \gamma_{th}\} = \int_0^{\gamma_{th}} f(\gamma) d\gamma \quad (6)$$

Where γ and γ_{th} are the instantaneous SNR of receive signal and SNR threshold, respectively. $f(\gamma)$ represents the probability density function of γ .

From equation (1), the instantaneous SNR and average SNR of the receive signal can be expressed as $\gamma = \eta^2 h^2 I^2 / 2\sigma_n^2$ and $\bar{\gamma} = \eta^2 E[h]^2 I^2 / 2\sigma_n^2$. Then we can have that,

$$h = E[h] \sqrt{\frac{\gamma}{\bar{\gamma}}} \quad (7)$$

In order to obtain the probability density function of the instantaneous SNR in multi-user MRR laser communication system, the probability density function of system channel is firstly considered, which can be expressed as equation (8).

$$f(h) = f(h_a^{2N-1} h_{0,1} h_{1,2} \cdots h_{N-1,N} h_{N,N-1} \cdots h_{1,0}) = h_a^{2N-1} f(h_{0,1} h_{1,2} \cdots h_{N-1,N} h_{N,N-1} \cdots h_{1,0}) \quad (8)$$

For equation (8), the following substitution methods is considered.

$$\begin{aligned} \tilde{h}_1 &= h_a h_{0,1} h_{1,2} \\ \tilde{h}_{m+1} &= \begin{cases} h_a \tilde{h}_m h_{m+1,m+2} & 0 < m < N-1 \\ h_a \tilde{h}_m h_{2N-m-1,2N-m-2} & N-1 \leq m \leq 2N-2 \end{cases} \\ \tilde{h}_{2N-1} &= h \end{aligned} \quad (9)$$

With mathematics induction, the probability density functions of $\tilde{h}_1, \tilde{h}_{m+1}$ and \tilde{h}_{2N-1} are considered. For \tilde{h}_1 , as it has a connection with $h_{0,1}$ and $h_{1,2}$, the joint probability density function of $h_{0,1}$ and $h_{1,2}$, $f_{h_{0,1},h_{1,2}}(h_{0,1}, h_{1,2})$, is considered. According to the irrelevance between $h_{0,1}$ and $h_{1,2}$, $f_{h_{0,1},h_{1,2}}(h_{0,1}, h_{1,2})$ can be expressed as follow,

$$f_{h_{0,1},h_{1,2}}(h_{0,1},h_{1,2}) = f_{h_{0,1}}(h_{0,1})f_{h_{1,2}}(h_{1,2}) \quad (10)$$

With $h_{1,2} = \tilde{h}_1/h_a h_{0,1}$, we can have that,

$$f_{\tilde{h}_1,h_{0,1}}(\tilde{h}_1,h_{0,1}) = \frac{1}{h_a h_{0,1}} f_{h_{0,1}}(h_{0,1})f_{h_{1,2}}\left(\frac{\tilde{h}_1}{h_a h_{0,1}}\right) \quad (11)$$

Integrate $h_{0,1}$ at both ends of equation (11) and use equation (3). We can have that,

$$\begin{aligned} f(\tilde{h}_1) &= \int_0^\infty f_{\tilde{h}_1,h_{0,1}}(\tilde{h}_1,h_{0,1})dh_{0,1} = \frac{1}{h_a} \int_0^\infty \frac{1}{h_{0,1}} f_{h_{0,1}}(h_{0,1})f_{h_{1,2}}\left(\frac{\tilde{h}_1}{h_a h_{0,1}}\right)dh_{0,1} \\ &= \frac{1}{\Gamma(\alpha_{0,1})\Gamma(\beta_{0,1})\Gamma(\alpha_{1,2})\Gamma(\beta_{1,2})\tilde{h}_1} G_{0,4}^{4,0}\left(\frac{\alpha_{0,1}\beta_{0,1}\alpha_{1,2}\beta_{1,2}}{h_a} \tilde{h}_1 \mid \alpha_{0,1}, \beta_{0,1}, \alpha_{1,2}, \beta_{1,2}\right) \end{aligned} \quad (12)$$

where $G_{p,q}^{m,n}(z)$, $m, n, p, q \in \mathbb{N}$, $m \leq q$, $n \leq p$ is stand for Meijer-G function, which is defined as follow,

$$G_{p,q}^{m,n}\left[z \mid \begin{matrix} a_1, \dots, a_n, a_{n+1}, \dots, a_p \\ b_1, \dots, b_m, b_{m+1}, \dots, b_q \end{matrix}\right] = \frac{1}{2\pi i} \int_L \frac{(\prod_{k=1}^m \Gamma(s+b_k)) \prod_{k=1}^n \Gamma(1-a_k-s)}{(\prod_{k=n+1}^p \Gamma(s+a_k)) \prod_{k=m+1}^q \Gamma(1-b_k-s)} z^{-s} ds \quad (13)$$

There is an equivalence relation between Meijer-G function and the second-class Bessel function as follow,

$$K_\nu(z) = \frac{1}{2} G_{0,2}^{2,0}\left(\frac{z^2}{4} \mid \nu, -\nu\right) \quad (14)$$

The result of equation (12) can be obtained by substituting equation (14) into the derivation process of equation (12).

The probability density functions of \tilde{h}_{m+1} and \tilde{h}_{2N-1} can be obtained by steps similar to equations (10)~(12), and the specific form is as follows.

$$f(\tilde{h}_{m+1}) = \frac{1}{A \tilde{h}_{m+1}} G_{0,2m+4}^{2m+4,0} \left(\frac{B}{h_a^{m+1}} \middle| \begin{matrix} - \\ C \end{matrix} \right)$$

$$\left\{ \begin{array}{l} A = \prod_{k=0}^{m+1} \Gamma(\alpha_{k,k+1}) \Gamma(\beta_{k,k+1}); \\ B = \prod_{k=0}^{m+1} \alpha_{k,k+1} \beta_{k,k+1}; \quad 0 < m < N-1 \\ C = \alpha_{0,1}, \beta_{0,1}, \alpha_{1,2}, \beta_{1,2}, \dots, \alpha_{m+1,m+2}, \beta_{m+1,m+2}; \end{array} \right.$$

$$\left\{ \begin{array}{l} A = \prod_{k=0}^{N-1} \Gamma(\alpha_{k,k+1}) \Gamma(\beta_{k,k+1}) \prod_{k=N}^{m+1} \Gamma(\alpha_{2N-k,2N-k-1}) \Gamma(\beta_{2N-k,2N-k-1}); \\ B = \prod_{k=0}^{N-1} \alpha_{k,k+1} \beta_{k,k+1} \prod_{k=N}^{m+1} \alpha_{2N-k,2N-k-1} \beta_{2N-k,2N-k-1}; \quad N-1 \leq m \leq 2N-2 \\ C = \alpha_{0,1}, \beta_{0,1}, \dots, \alpha_{N-1,N}, \beta_{N-1,N}, \alpha_{N,N-1}, \beta_{N,N-1}, \dots, \alpha_{2N-m-1,2N-m-2}, \beta_{2N-m-1,2N-m-2} \end{array} \right.$$
(15)

$$f(h) = f(\tilde{h}_{2N-1}) = \frac{1}{h \prod_{k=0}^{N-1} (\Gamma(\alpha_{k,k+1}) \Gamma(\beta_{k,k+1}) \Gamma(\alpha_{k+1,k}) \Gamma(\beta_{k+1,k}))} \times$$

$$G_{0,4N}^{4N,0} \left(\frac{\prod_{k=0}^{N-1} \alpha_{k,k+1} \beta_{k,k+1} \alpha_{k+1,k} \beta_{k+1,k}}{h_a^{2N-1}} h \middle| \begin{matrix} - \\ \alpha_{0,1}, \beta_{0,1}, \alpha_{1,0}, \beta_{1,0}, \dots, \alpha_{N-1,N}, \beta_{N-1,N}, \alpha_{N,N-1}, \beta_{N,N-1} \end{matrix} \right)$$
(16)

According to equation (16), together with $h = E[h] \sqrt{\gamma/\bar{\gamma}}$ and $P_Y(y) = P_X(h(y)) |h'(y)|$, the probability density function, $f(\gamma)$, can be obtained by variable replacement, and can be expressed as follow,

$$f(\gamma) = \frac{1}{2\gamma A_0} G_{0,4N}^{4N,0} \left(\frac{B_0}{h_a^{2N-1}} E[h] \sqrt{\frac{\gamma}{\bar{\gamma}}} \middle| \begin{matrix} - \\ C_0 \end{matrix} \right)$$

$$A_0 = \prod_{k=0}^{N-1} (\Gamma(\alpha_{k,k+1}) \Gamma(\beta_{k,k+1}) \Gamma(\alpha_{k+1,k}) \Gamma(\beta_{k+1,k}))$$

$$B_0 = \prod_{k=0}^{N-1} \alpha_{k,k+1} \beta_{k,k+1} \alpha_{k+1,k} \beta_{k+1,k}$$

$$C_0 = \alpha_{0,1}, \beta_{0,1}, \alpha_{1,0}, \beta_{1,0}, \dots, \alpha_{N-1,N}, \beta_{N-1,N}, \alpha_{N,N-1}, \beta_{N,N-1}$$
(17)

As each forward link and backward link in the system are independent and irrelevant, the value of $E[h]$ in equation (17) can be calculated as follow,

$$E[h] = h_a^{2N-1} \prod_{k=0}^{N-1} E[h_{k,k+1}] E[h_{k+1,k}]$$
(18)

Considering the expectations of $h_{k,k+1}$ and $h_{k+1,k}$, we can have that,

$$E[h_{i,j}] = \int h_{i,j} f(h_{i,j}) dh_{i,j} = \frac{1}{\Gamma(\alpha_{i,j})\Gamma(\beta_{i,j})} \int G_{0,2}^{2,0}(\alpha_{i,j}\beta_{i,j}h_{i,j} | \alpha_{i,j}, \beta_{i,j}) dh_{i,j} = 1 \quad (19)$$

From equation (18) and (19), it can be known that $E[h] = h_a^{2N-1}$. Substituting this result into equation (17), it can be obtained that,

$$f(\gamma) = \frac{1}{2\gamma A_0} G_{0,4N}^{4N,0} \left(B_0 \sqrt{\frac{\gamma}{\bar{\gamma}}} \middle| C_0 \right) \quad (20)$$

Substituting the result in equation (20) into equation (6), the outage probability of multi-user MRR laser communication system can be obtained as follow,

$$P_{out} = \int_0^{\gamma} f(\gamma) d\gamma = \frac{1}{A_0} G_{1,4N+1}^{4N,1} \left(B_0 \sqrt{\frac{\gamma_{th}}{\bar{\gamma}}} \middle| C_0, 0 \right) \quad (21)$$

From equation (21), it can be known that the outage probability of multi-user MRR laser communication system is subject to average SNR, $\bar{\gamma}$, SNR threshold, γ_{th} , and large-scale fading coefficient and small-scale fading coefficient of the Gamma-Gamma model, $\alpha_{i,j}, \beta_{i,j}, \forall i, j$, and it is independent of other parameters in the system.

4. SIMULATION AND ANALYSIS

In this section, the outage probability of multi-user MRR laser communication with different SNRs, communication distances is compared by Monte-Carle method. The system parameters used in the simulation is shown in Table 1.

Table 1. System Parameters

Parameter	Value
Cycle Times N_n	10^6
Laser wavelength λ	1550nm
Atmospheric refractive index structure constant C_n^2	$1.7 \times 10^{-14} m^{-2/3}$
Laser transmitting aperture	0.02m
Laser receiving aperture	0.02m

Firstly, the scene with one receiver is considered. The relationship between outage probability of MRR laser communication system and communication distance is shown in Figure 3.

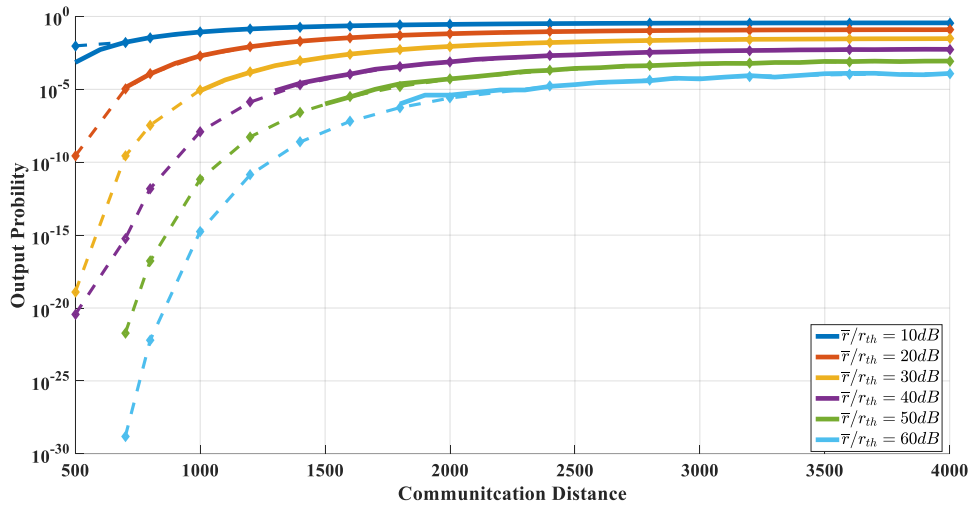


Figure 3. The relationship between outage probability of MRR laser communication system and communication distance

In Figure 3, the solid line data is the Monte Carlo simulation results, and the dotted line data is the calculation results of equation (21). The simulation results are highly consistent with the numerical calculation results. From Figure 3, it can be known that for different values of $\bar{\gamma}/\gamma_{th}$, the system outage probability is always increasing with the increase of communication distance, and the result is consistent with the performance degradation of the communication system as the communication distance becomes longer. Compared the system outage probability with different values of $\bar{\gamma}/\gamma_{th}$, it can be known that while $\bar{\gamma}/\gamma_{th} = 10dB$, the system outage probability is 10^{-3} with the communication distance 500m, and the system outage probability is larger than 0.1 with the communication distance longer than 1000m, which is unable to meet system communication requirements. While $\bar{\gamma}/\gamma_{th} = 50dB$, the system outage probability can maintain at the order of 10^{-3} with the communication distance 4000m.

Secondly, the system outage probability under the influence the receiver number is considered when the communication distance between each receiver is fixed at 1000m

The simulation result is shown in Figure 4.

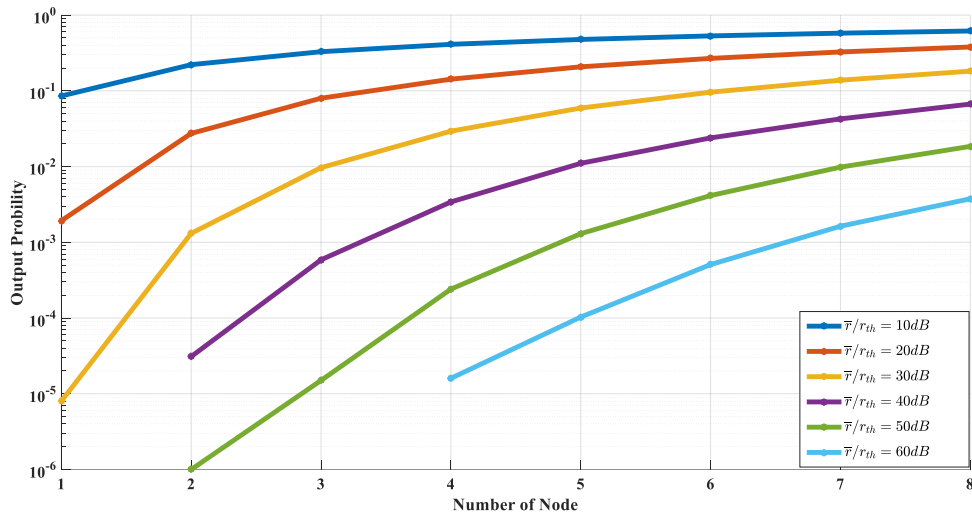


Figure 4. The relationship between system outage probability and receiver number when the communication distance is fixed at 1000m

From Figure 4, it can be known that when the receiver number increases, the total communication distance becomes longer, and the system outage probability has an increase, which is consistent with the results in Figure 3. There are two factors, communication distance and multi-user laser communication mode, that have an influence on system outage probability. Contrasting Figure 3 and Figure 4, it can be found that with the same total communication distance, the system outage probability of single-user and multi-user is similar. When the communication distance is 1000m, the communication distance is the main factor affecting outage probability. In order to discuss the impact of the multi-user laser communication model further, the simulation in Figure 5 is carried out.

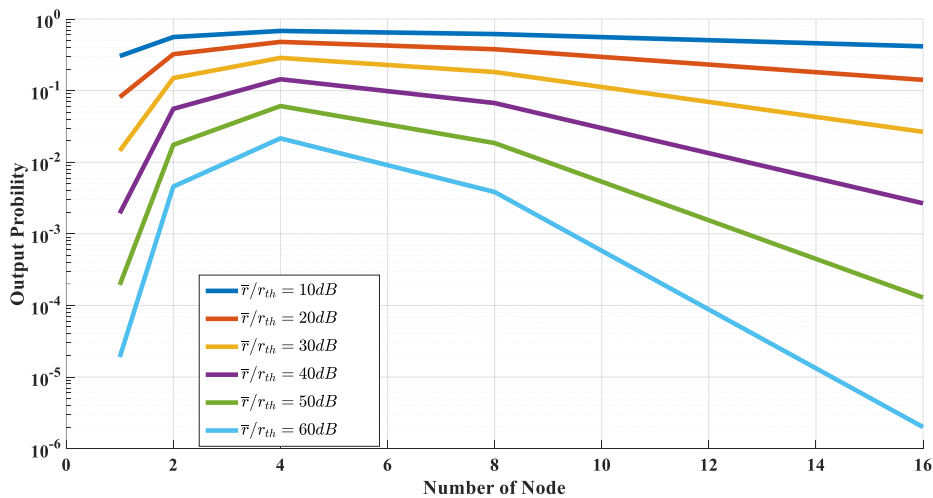


Figure 5. The relationship between system outage probability and receiver number when the total communication distance is fixed. In Figure 5, the total communication distance is 8000m, and the receiver number is adjusted while ensuring the same communication distance between receivers. For example, if there is N receivers in the system, the communication distance

between receivers is $(8000/N)m$. From Figure 5, it can be known that while the communication distance between receivers is shorter than 2000m, the system outage probability increases with the increase of communication distance, and conversely, the system outage probability decreases with the increase of communication distance while the communication distance is longer than 2000m. When the communication distance between receivers is equal to 2000m, the system outage probability influenced by communication distance and relay times reaches the maximum value. Then, it can be inferred that as the total communication distance is fixed and the receiver number become larger, the system outage probability can be reduced when the communication distance is shorter than the threshold(2000m). What's more, when the value of $\bar{\gamma}/\gamma_{th}$ is small, the outage probability of multi-user laser communication system is inferior to that of single-user laser communication system although the communication distance is as short as 500m. However, when the value of $\bar{\gamma}/\gamma_{th}$ is large, the outage probability of multi-user laser communication system can be better than that of single-user laser communication system as the communication distance become shorter.

5. CONCLUSION

In this paper, the performance of multi-user MRR laser communication system in atmospheric turbulence fading is studied. The closed form solution of the system outage probability is analyzed by derivation and simulation. From the simulation results, the optimal receiver number and communication distance of multi-user MRR laser communication system in different scenarios is discussed, which can guide the parameter setting in multi-user MRR laser communication system and be the basis for optimizing the performance of multi-user MRR laser communication system. How the large-scale fading coefficient and small-scale fading coefficient in atmospheric turbulence fading are affected by system parameters and their influence on system outage probability can be studied for future work.

REFERENCE

- [1] Jiang S , Zhang M . Research on the Performance of Free Space Optical Communications Systems under Weak Turbulence[J]. Information & Communications, 2019.
- [2] Ciftcioglu B . Intra-Chip Free-Space Optical Interconnect: System, Device, Integration and Prototyping.[D]. University of Rochester. 2012.
- [3] Khan M , Chakareski J . Neighbor Discovery in a Free-Space-Optical UAV Network. 2019..
- [4] Plank T, Leitgeb E, Loeschnigg M. Recent developments on free space optical links and wavelength analysis[C], In Proceedings of Space Optical Systems and Applications (ICSOS), pp. 14-20, 2011.
- [5] Wang J , Wang Y , Gao C , et al. Properties of cat-eye modulating retro-reflector and its application with piezoelectric transducer[J]. Optik - International Journal for Light and Electron Optics, 2014.
- [6] Wang K , Xu Z , Li X , et al. Analysis of space diversity method in modulating retro-reflector optical communication[J]. Editorial Office of Opto-Electronic Engineering, 2020(03).
- [7] Qiu H , Wang J Y , Zhi-Yong X U , et al. Modulating Retro-reflector Optical Communication Technology[J]. Journal of Military Communications Technology, 2015.

- [8] Ninos M P , Nistazakis H E , Tombras G S . On the BER performance of FSO links with multiple receivers and spatial jitter over gamma-gamma or exponential turbulence channels[J]. *Optik - International Journal for Light and Electron Optics*, 2017.
- [9] Kaushal H, Kaddoum G. Optical communication in space: challenges and mitigation techniques[J]. *IEEE Communications Surveys & Tutorials*, 2016, 19(1): 57-96.
- [10] Bashir M S , Alouini M S . Optimal Power Allocation Between Beam Tracking and Symbol Detection Channels in a Free-Space Optical Communications Receiver[J]. *Institute of Electrical and Electronics Engineers (IEEE)*, 2021(11).
- [11] Quintana C , Wang Q , Jakonis D , et al. A High Speed Retro-Reflective Free Space Optics Links With UAV[J]. *Journal of Lightwave Technology: A Joint IEEE/OSA Publication*, 2021(39-18).
- [12] Two-dimension image construction for range-resolved reflective tomography Laser radar[C]// *Conference on free-space and atmospheric laser communications XI. Key Laboratory of Space Laser Communication and Testing Technology, Shanghai Institute of Optics and Fine Mechanics, Chinese Academy of Sciences, P. O. Box 800-211, Shanghai 201800, P. R. China; Key Laboratory of Space Laser Communication and Testing Technol*, 2012.
- [13] Pasupathi T , Selvi J . Design, Testing and Performance Evaluation of Beam Positioning System for Free Space Optical Communication System[J]. *Brno University of Technology*, 2021(1).
- [14] Samimi, H., Uysal, M.: 'End-to-end performance of mixed RF/FSO transmission systems', *IEEE/OSA J. Opt. Commun. Netw.*, 2013, 5, (11), pp. 1139–1144.
- [15] Yang G, Li C, Li J, et al. Performance analysis of full duplex modulating retro-reflector free-space optical communications over single and double gamma-gamma fading channels[J]. *IEEE Transactions on Communications*, 2018, 66(8): 3597-3609.
- [16] Zhang L X , Sun H Y , Zhao Y Z , et al. Effect of the incidence angle to free space optical communication based on cat-eye modulating retro-reflector[C]// *Society of Photo-Optical Instrumentation Engineers (SPIE) Conference Series. SPIE*, 2013.